Appl Phys B (2009) 96: 401–408
DOI 10.1007/s00340-009-3539-3

Applied Physics B
Lasers and Optics

Adaptation to the edge of chaos in a self-starting Kerr-lens mode-locked laser

C.C. Hsu · J.H. Lin · W.F. Hsieh

Received: 8 December 2008 / Revised version: 9 March 2009 / Published online: 2 May 2009

Abstract We experimentally and numerically demonstrated that self-focusing acts as a slow-varying control parameter that suppresses the transient chaos to reach a stable mode-locking (ML) state in a self-starting Kerr-lens mode-locked Ti:sapphire laser without external modulation and feedback control. Based on Fox–Li's approach, including the self-focusing effect, the theoretical simulation reveals that the self-focusing effect is responsible for the self-adaptation. The self-adaptation occurs at the boundary between the chaotic and continuous output regions in which the laser system begins with a transient chaotic state with fractal correlation dimension, and then evolves with reducing dimension into the stable ML state.

PACS 42.60.Mi · 42.65.Sf · 42.65.Re · 05.45.Gg · 05.45.Pq

1 Introduction

A self-adapting or self-adjusting system is an adjustable system whose control parameters are adjusted by the forcing dependent only on the system itself [1]. Such systems have been found to adapt to the edge of chaos, which is the boundary of chaos and the ordered state [1, 2]. Using the logistic map as an example [1], it had been found that the parameter leaves the chaotic regime and there is a high probability of finding the parameter at the boundary between periodicity and chaos when the control parameter of the system is not constant in time but varies much more slowly than the dynamical variables. These phenomena are ubiquitous in nature; for example, long-range fitness correlations have been detected during the adaptive process in RNA viruses [3]. In addition, models of coupled neurons with self-adjusting coupling strengths had been found to exhibit robust synchronization [4] and suppression of chaos [5].

Since the laser came on the scene, the rich nonlinear dynamics has been investigated intensively in laser systems. Typically, if only one spatial mode of the electromagnetic field is excited in the laser, the interesting instabilities are temporal [6]. Nevertheless, under some circumstances, parameters can be adjusted so that more spatial modes come into play and spatio-temporal instabilities [7] also appear. Lugiato et al. expressed the Maxwell–Bloch equations in terms of modal amplitudes by using a suitably cylindrically symmetric empty-cavity-mode expansion [8, 9]. They presented various spatiotemporal instabilities, including chaos and cooperative frequency locking, which occur under uniform pumping with the pump size being larger than the minimum cavity beam waist [10].

By using Greene's residue theorem [11] to analyze the iterative map of a Gaussian beam q parameter of a general optical resonator [12], we found that, even when only fundamental mode propagation is considered, some specific configurations that have so-called low-order resonance [11] may become unstable under the influence of persistent nonlinear effects [12–14]. When the pump size is smaller than the

C.C. Hsu · W.F. Hsieh (✉)
Department of Photonics and Institute of Electro-Optical Engineering, National Chiao Tung University, 1001 Tahsueh Rd., Hsinchu 300, Taiwan
e-mail: wfhsieh@mail.nctu.edu.tw

J.H. Lin
Department of Electro-Optical Engineering & Institute of Electro-Optical Engineering, National Taipei University of Technology, 1, Sec. 3, Chung-Hsiao E. Rd., Taipei 106, Taiwan

W.F. Hsieh
Institute of Electro-Optical Science and Engineering, National Cheng Kung University, 1 University Rd., Tainan 710, Taiwan

waist of the cold cavity in axial-continuously (CW) pumped solid-state lasers, peculiar lasing behavior [15–19] has been observed near the degenerate configurations that correspond to the low-order resonance. At these degenerate cavity configurations, a supermode or superposition of phase-locked degenerate transverse modes can be formed with relatively low lasing threshold, shrunken beam waist [16] and operation of a stable CW bottle beam [17, 18] were observed. However, only the temporal chaotic state was observed for the cavity configurations that were slightly shorter than the degenerates and the spatio-temporal chaotic state for those slightly longer than the degenerates [19].

The chaotic behavior had been studied in mode-locked gas lasers such as He–Ne laser [20] and NH_3 laser [21]. In solid-state mode-locked (ML) lasers, the chaotic behavior of the self-mode-locking or the Kerr-lens mode-locking (KLM) Ti:sapphire lasers, due to the significant optical Kerr effect (OKE), had also been investigated since the invention of KLM Ti:sapphire laser in 1991 by Spence et al. that requires a mechanical perturbation to start the mode locking [22]. Later, self-starting Kerr-lens mode locking (SSKLM) was shown achievable in this laser, either with or without group velocity compensation [23, 24] in a narrower tuning region close to the boundary of spatio-temporal chaotic and CW states [25]. The basic mechanism underlying pulse formation in these self-mode-locked lasers has been attributed to self-focusing caused by Kerr nonlinearity to modulate the cavity gain or loss in terms of soft-aperture or hard-aperture Kerr-lens mode locking [26, 27], respectively. For soft-aperture systems, however, because the only mechanism to restrict higher-order transverse modes is the modal profile of the gain and because Kerr-lens mode locking itself is intrinsically a nonlinear phenomenon, it is not surprising that such systems may exhibit a more complicated transverse dynamics. Recently, period doubling [28, 30] and tripling [29, 30] of soft-aperture Kerr-lens mode-locked Ti:sapphire lasers were observed by operation of the resonators in specific cavity configurations and were explained in terms of the total mode locking of TEM_{00} and higher-order modes [31, 32].

Although the dynamic processes of the self-starting KLM lasers have been extensively investigated in early time in which starting from relaxation oscillation through a short period intermediate free running to reach a final stable KLM were generally reported [33], many efforts concerning the routes to chaos after the lasers had been operated with the KLM state were reported, e.g., Bolton et al. [34], and our previous report [25]. A phase plot of period, quasiperiodic, and chaotic regimes shows as a function of pump power and insertion of prism [26]. However, to the best of our knowledge, self-adaptation from transient spiking to complete mode locking with neither external modulation [35–37] nor feedback control [38–40] had not been examined in laser systems. In this article, we will report the experimental demonstration in laser systems in which the dynamic processes of self-starting KLM begin with the transient chaotic state and finally suppression of chaos to become a stable CW-ML state. Based on the Fox–Li approach, including the self-focusing effect, the simulation results reveal that the self-focusing effect is responsible for the dynamics of this laser system that evolves from the chaotic state with a strange attractor to a metastable periodic state and then converges to a fixed point, the CW-ML state.

2 Experimental setup

The experiment setup of picosecond (ps) Ti:sapphire laser is shown in the inset of Fig. 1. An all line Ar-ion laser was used to pump a Brewster-angle cut Ti:sapphire laser rod with

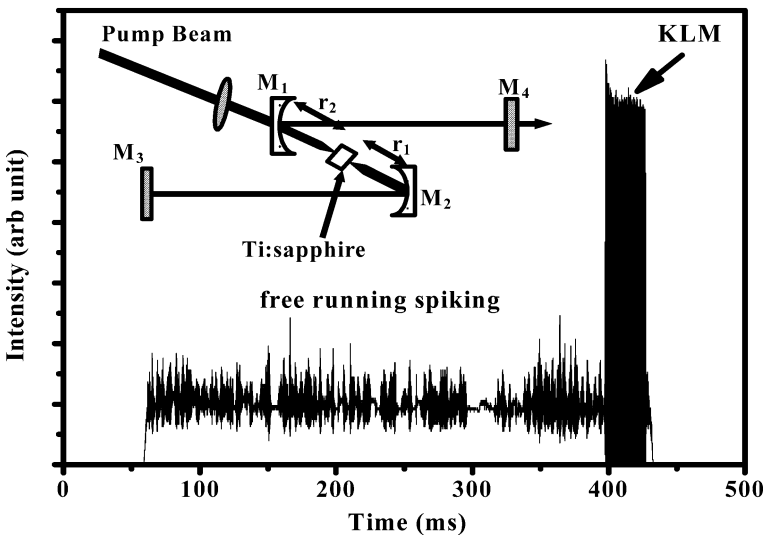

Fig. 1 The output clusters of the self-starting pulse train on the oscilloscope with 5 W pump. The CW laser oscillated with free running spiking when the cavity path was unblocked and then suddenly broke into KLM operation. The *inset* is the experiment setup of a picosecond pulse Ti:sapphire laser

length $l = 9$ mm. Without any GVD compensation, the single pass GVD for the 9 mm Ti:sapphire crystal is 576 fs^2. A Z-shaped resonator consists of two curved mirrors, M_1 and M_2, with the radius of curvature $R = 10$ cm, and two output couplers, M_3 and M_4, having transmissions of 2 and 5 percent, respectively. The distance from M_1 to one end face of the laser rod is denoted as r_2, and from the other end face to M_2 as r_1. In a near-symmetric arrangement, the distance d_2 from the output coupler M_3 to M_2 is equal to the distance d_1 from M_4 to M_1. By properly adjusting the cavity configuration we obtained self-starting KLM lasing [23, 25] that can be operated for a long period of time. We measured the stable KLM pulse having the pulse width of about 3 ps. The output from M_3 was detected by high-speed silicon PIN diodes (Electro-Physics Technology ET 2000, with 300-ps rise time) and then connected to a 300-MHz digital oscilloscope (LeCroy 9450A) used to monitor and store the dynamic of laser for further analysis. The self-starting was examined by blocking and unblocking the cavity beam to observe whether the laser will self-develop into the KLM state or not. We found the self-starting will always occur after the cavity beam is unblocked.

3 Results and discussion

Figure 1 shows the typical evolving output of the self-starting KLM laser developed from spontaneous noise under 5W CW pumping. Apparently, the laser first oscillated with free running spiking once the cavity path was unblocked. It then evolved into stable KLM operation with a pulse width of 3 ps. To verify the determinism of the data, the correlation function and the correlation dimension proposed by Grassberger-Procaccia analysis (GPA) [41] were applied.

To do the GPA, the time embedding technique is required to construct the trajectory in the D_e embedding dimensions with a vector y_i. The number of pairs of points with a separation distance less than some value r is estimated by

$$C(r) = \lim_{N\to\infty} \frac{2}{(N - D_e + 1)(N - D_e)} \times \sum_{i}^{(N-D_e+1)} \sum_{j>i}^{(N-D_e+1)} H\big(r - (y_i - y_j)\big), \quad (1)$$

where y_i and y_j are the coordinates of the ith and jth vectors of total N data, and H is the Heaviside function, which is defined as $H(u) = 1$ if $u > 0$, but zero otherwise. The distance r can be simply a Euclidean norm. Because $C(r)$ could vary as $C(r) \approx r^d$, where d is the dimension of the attractor, by the slope of the $\log[C(r)]$ versus $\log(r)$ plot it is possible to determine d if we have the correct minimum embedding dimension whose slope would convert to a value despite choosing the greater values of D_e.

The measured data in the experiment are continuous or represented a discrete time sequence of laser outputs $x(t)$, recorded by an oscilloscope with a sampling interval of τ, and represented by $x(\tau_0 + n\tau)$ or x_n. For the nonlinear dynamic analysis, we have reported detailed bifurcation diagrams and verified the determinism of the chaotic state in the soft-aperture KLM [25]. Here we used 30,000 data points of transient irregularity with 0.01 ms sampling time before the complete KLM. Figure 2 shows the slope of $\log[C(r)]$ versus $\log(r)$ for the embedding $D_e = 2$ to 12. When the length scales are smaller than or equal to the noise strength, the noise will cause fuzziness so that we would recognize only $C(r) \approx r^d$ for $r > r_{\text{noise}}$. This value d increases until it reaches a constant value as the embedding dimension D_e is large enough to accommodate the attractor. A plateau can be seen within proper length scale in Fig. 2 with a finite and non-integer value of $d = 2.11 \pm 0.08$, indicating the transient irregularity is chaotic. The chaotic characteristic can

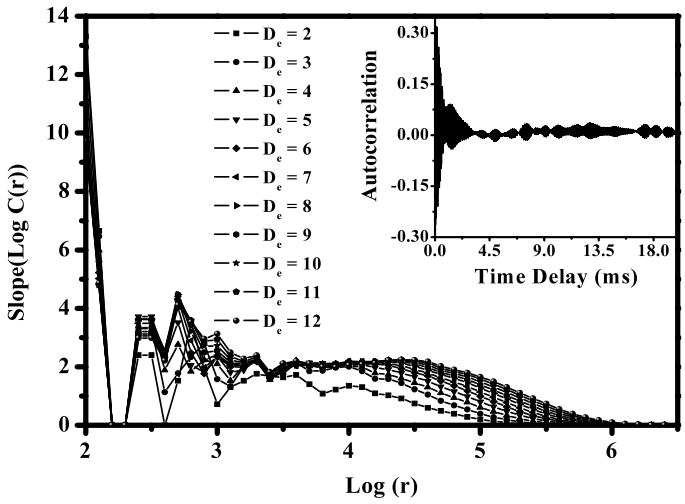

Fig. 2 The calculated log $[C(r)]/\log(r)]$ versus $\log(r)$ with embedding dimension D_e from 2 to 12 by the GPA. The *inset* is the damped autocorrelation that reveals a chaotic characteristic

be confirmed further by observing the revivals of the autocorrelation function for a long delay time, as shown in the inset of Fig. 2.

The laser instabilities, e.g., the instabilities of single mode [42] and multimode [43, 44] lasers and transverse instabilities [45], are generally described by Maxwell–Bloch equations. However, since the Ti:sapphire laser is a class B laser, the polarization relaxation rate is faster than those of field and population, and the Maxwell-Bloch equations are reduced to the rate equation. Furthermore, in the passive mode-locked laser, the OKE can be exploited to simulate the fast saturable absorber behavior and the rate-equation approach can describe sufficiently the transmission of an optical pulse through such a fast saturable absorber without using more complex resonant-dipole or Rabi-flopping analyses [46]. For comparison with the experimental observation, and to ascertain that the chaotic characteristic is a result of the self-focusing effect, we numerically simulated this laser system by using Collin's integral [47] with round-trip transmission matrix to calculate the light field $E(r)$ under cylindrical symmetry, where r is for the corresponding radial coordinates and the rate equations are as described in our previous work [48], in which the gain coefficient is expressed as

$$g_{m+1} = (1-\gamma_a \Delta t) g_m + \frac{2\Delta t}{h\nu_p N_0 l}\left(\frac{P_p}{\pi w_p^2} e^{\frac{-2r^2}{w_p^2}}\right)(\sigma N_0 - g_m) - \frac{\gamma_a \Delta t}{|E_s|^2}|E_m|^2 g_m. \quad (2)$$

Here we used the spontaneous decay rate $\gamma_a = 3.125 \times 10^5$ s^{-1} [49], the total density $N_0 = 3.3 \times 10^{25}$ m^{-3} [49], the length $l = 9$ mm, the stimulated-emission cross section $\sigma = 3.0 \times 10^{-23}$ m^2 [50], and the saturation parameter $E_s = 1.05 \times 10^6$ NC^{-1} [50] of the active medium; and the round trip time $\Delta t = 10.67$ ns, determined by cavity length, the photon energy of the pumping laser $h\nu_p = 1.53$ eV, pumping beam radius $w_p = 15$ μm in the gain medium, and $P_p = 5$ W is the effective pumping power. Notice that the mode-locking mechanism in a Kerr-lens mode-locking laser is due to the self-amplitude or self-gain modulation resulting from the self-focused light by the hard- or soft-aperture effect. Therefore, the pumping beam radius w_p must be smaller than the cold cavity beam radius w_c (∼25 μm) in the gain medium leading to the KLM mode to resonate more easily than the CW mode. We have omitted the dispersion of the active medium, so that the gain is assumed to be real. The filtering mechanism from the loss difference [51, 52] need not be considered because the gain band width of the picosecond pulses is much smaller than the band width of the mirror reflectance.

In order to include the self-focusing effect in active medium, we modified the equation to describe the light field passing through the gain medium by adding the nonlinear phase shift caused by OKE as

$$\phi(r) = \frac{2\pi}{\lambda} n_2 l I(r) \quad (3)$$

in the evolution equation of the light field

$$E_+^m = E_-^m \exp\left(\frac{1}{2} g_m l - i\phi\right) + E_{\text{spont}}^m. \quad (4)$$

Here E_-^m and E_+^m are the electric fields of the m-th round trip just reaching and leaving the laser rod; l is the length of gain medium; E_{spont}^m is the field of spontaneous emission whose amplitude is given by the spontaneous decay term in (2) and a phase obtained from a random generator; and n_2 is the nonlinear refractive index. $I(r)$ is the intensity distribution of laser pulse calculated from the electric field $E_-^m(r)$ using $I(r) = (1/2n\varepsilon_0)|E_-^m(r)|^2$, where n is the refractive index and ε_0 is the permittivity of free space. A similar treatment is for the opposite direction propagation. The processes repeat in each round trip until they reach convergence to a continuous-wave steady state for the CW laser output.

When we omit the self-focusing effect, i.e., $\phi = 0$ in (4), the model had been used for a description as the laser dynamics involving the interplay of beam propagation and gain dynamics as cavity is tuned toward the degeneration [48]. However, if we considered the self-focusing effect, it modifies the wave front of the propagation field according to (4) through the beam propagation described by the diffraction integral. The spot size of the electric field will shrink in every trip through the gain medium. The smaller pumped spot size than the cold cavity one causes the KLM state to have a better overlap integral than the CW state to extract more stored gain. Although the self-focusing effect is considered instantaneous to modify the beam profile, the resultant electric field distribution would be governed by gain dynamics, which has a recovery time of 3.2 μs and is a relatively slow process.

In order to investigate the cavity-dependent instability, we varied r_1, which changes the electric field distribution in the gain medium corresponding to influence optical Kerr effect on laser dynamics, across the point of degeneration, and set the initial values of $E(r)$ to zero, i.e., $E_-^1(r) = 0$, to calculate the output power. Here setting the initial values of $E(r) = 0$ is to avoid the value of stable output field at position r_1 substituting the initial value at the next position of r_1. The real initial condition is the spontaneous-emission noise rather than "the zero field value". The zero solution is also a trivial solution. All parameters and variables used in the program have been set at double precision.

Without considering OKE ($n_2 = 0$), typical laser output begins with a relaxation oscillation and then a stable output in all the stable cavity configurations [48]. Let $n_2 =$

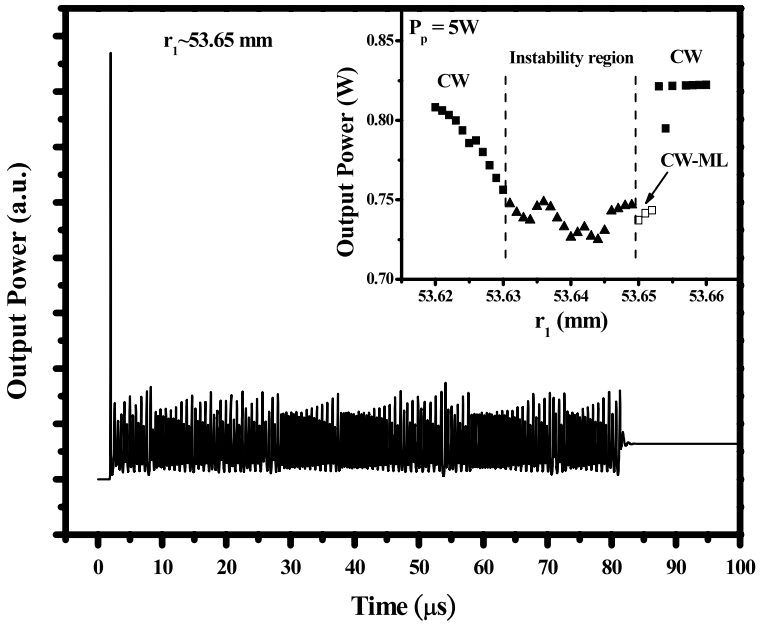

Fig. 3 The simulation results of the laser output power around the degenerate cavity configuration. A large fluctuation is similar to the situation of the transient irregular spiking before the KLM as shown in Fig. 1. The *inset* is the lasing states versus cavity tuning, where r_1 is the distance between the curved mirror M_2 and the end face of the laser crystal

3×10^{-20} m^2 W^{-1} and pulsewidth $\tau_p = 3$ ps; the laser output states versus the tuning range are shown in the inset of Fig. 3. The stable laser output after the relaxation oscillation can be seen in the CW regions. However, instability output can be seen as the cavity configuration tuned close to the degenerate cavity configurations, set here around 1/3-transverse degeneracy, in which the transverse modes with mode numbers $m + n = 3N$ have the same frequency as the fundamental mode, where N is an integer.

The laser is situated either quasi-periodic or chaotic between $r_1 = 53.63$ and 53.65 mm (solid triangles), e.g., they are completely chaotic at $r_1 = 53.64$ mm and operated at CW state (solid squares) after transient oscillation for $r_1 <$ 53.63 mm and $r_1 > 53.655$ mm. It is worth noting that the simulated SSKLM output as shown in Fig. 3, which is operated at CW-ML state (open squares), is similar to the experimental one (see Fig. 1), which possesses transient irregularity before reaching a constant output at $r_1 = 53.65$ mm. However, we cannot determine directly whether the constant output is completely KLM or CW output, due to lack of temporal information within a round trip time. By analyzing the simulated data in this case, we also obtained a similar decaying correlation function as the results of analyzing the experimental data in Fig. 2, with correlation dimension of 1.67 ± 0.15. Furthermore, the simulated result shows that the CW-ML occurred at the edge of a power dip around a degenerate cavity configuration, and it also agrees with our experimental reports [30].

To investigate the evolution of the SSKLM laser from the transient chaos into complete mode locking, we divided the 30,000 transient irregularities of the experimental data points into five parts with 10,000 data points per section, but overlapping 5,000 data points with the successive sections to calculate the evolving of the correlation dimension. However, the pulse peak detection based on Bolton et al. [40] must be used for the data of the complete KLM pulses. We therefore recorded separately the successive mode-locking pulses during the complete KLM. We acquired each mode-locking pulse containing 5 to 6 points and a total of 3,500 pulses for this calculation. Each data point represents an accumulation over approximately 2 ns. The maximum value of the voltage on the oscilloscope, with 8-bit flash, was read as approximately 2 V for our measured pulse train [25]. Shown in Fig. 4(a), the correlation dimension initially is a non-integer 2.56 ± 0.17, and then declines gradually to an integer dimension of 1. Finally, it evolves to a periodic complete KLM state of $d = 0$. Correspondingly, for the simulation results, the correlation dimension evolves similarly from 1.88 to 1, then to $d = 0$. Furthermore, the characteristics of the phase space can be derived by a plot, named "return map," obtained from the time series that is the observed output of the dynamical system [53]. A return map of the simulated SSKLM result is shown in Fig. 4(b). It presents a strange attractor in the initial stage. With time evolution, the chaotic state transits to the quasi-periodic (metastable) state corresponding to $d = 1$ and then converges to a fixed point ($d = 0$).

Lasers are typical systems in which the "slaving principle" applies, as Haken [54] has elegantly explained. In general, any kind of laser can be described by means of a set of coupled non-linear differential equations involving the first-order time derivatives that can be represented as $\frac{d\vec{x}}{dt} = F_{\vec{\mu}}(\vec{x}, t)$. The time-dependence vector $\vec{x} = (x_1, \ldots, x_n)$ represents the n dynamical variables describing the laser system, so that its evolution defines a trajectory or orbit of the system in the phase space defined by these variables, and the

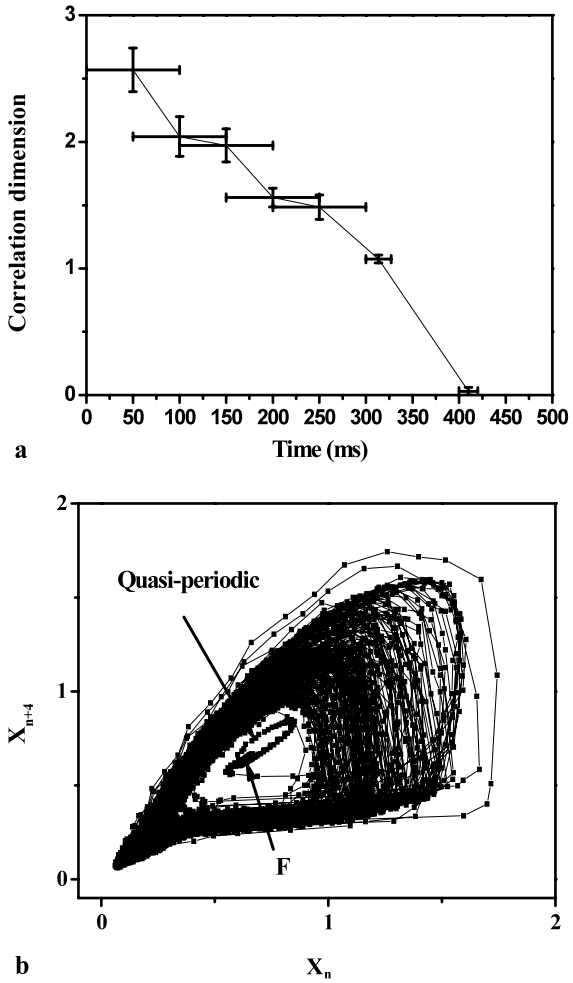

Fig. 4 The time evolution of the correlation dimension of the observed (**a**) and the return map of simulated output power (**b**). F: fixed point

vector field $F_{\vec{\mu}}$ describes the nonlinear coupling between the dynamical variables in a given kind of laser. Generally, $F_{\vec{\mu}}$ depend on several control parameters designated by a vector $\vec{\mu} = (\mu_1, \ldots, \mu_p)$ that characterizes each specific set of experimental conditions. If the control parameter μ_j is much larger than the remaining ones, the influenced variable x_j rapidly "loses" the memory of its history (i.e., of the values reached at preceding times); in such a way, it adapts rapidly to the instantaneous values reached by the remaining variables approximately proportional to μ_j. Therefore, the slowly evolving variables completely determine the evolution of the physical system. The self-focusing effect may play a role of slowly controlling the parameter to the studied laser system, and the slaving principle can be applied to describe the observed time evolving correlation dimension and the transient return map from the chaotic state to ML state.

In our previous reports, the laser dynamics are dependent on laser cavity configuration. The transverse-mode pattern is consisting of high-order transverse modes in a degenerate cavity configuration [30, 55]. Owing to the superposition of high-order modes, the transverse mode could be self-adjusted to match the pumping profile for extracting maximal pumped gain in cavity. The laser dynamics shows existence of temporal or spatial temporal instabilities when the nonlinear effects were in existence around the degenerate cavity configurations [48]. The Kerr-lens mode-locking in a Ti:sapphire laser is dependent on the cavity configuration, no matter whether it is operated in picosecond or femtosecond pulse [30]. The ML region, varying the distance between the mirror and the crystal, is ∼300 μm including the self-starting ML in smaller region ∼30 μm. When the mirror was tuned within 30 μm range, the laser parameters, such as the beam waist of the cold cavity, cavity loss, etc., would be unchanged but change in the relative Gouy phases of the transverse modes [18]. The pulse energy is fixed but waist is not, in a stable mode-locked laser.

It is known that, far from the threshold of continuous (supercritical) instability, only the phase of the complex field survives as a slow degree of freedom, since it describes the symmetry of the system [56]. Therefore, the nonlinear phase due to the nonlinear Kerr coefficient

$$\gamma = n_2/\left(n_0^3 A_{\text{eff}}\right) \tag{5}$$

may act as the slowly varying control parameter [1]. Here n_0 is the linear refractive index and A_{eff} is the effective area in the Kerr medium [57]. Because the optical field originates from the spontaneous emission whose spot size is approximately corresponding to the spot size of the pumped beam, which is smaller than the spot size of a cold cavity, the initial values of $1/A_{\text{eff}}$ are almost constant, which is equal to 1.4×10^{11} m^{-2} as shown by a dash line in Fig. 5. $1/A_{\text{eff}}$ calculated at $N = 10,000$ round trips is equal to 3×10^{11} m^{-2} at the CW-ML state, which is sandwiched between instability and CW regions in the inset of Fig. 3. By plotting the probability of finding $1/A_{\text{eff}}$ after 10,000 round trips as a function of γ in a wide cavity tuning range of 70 μm in Fig. 5, we found γ does adapt to the edge of chaos that has the highest probability.

4 Conclusion

Without external modulation and feedback control, we have observed self-starting Kerr-lens mode locking with picosecond pulses in the Ti:sapphire laser. From the decay autocorrelation function with long time revival, and the fractal correlation dimension for the transient irregularity of the laser output before the complete mode locking, we ascertained that the SSKLM is initially at the chaotic state. Based on the Fox–Li approach, including the self-focusing effect, the simulation results reveal that the self-focusing effect is responsible for the dynamics of this laser system that evolves from

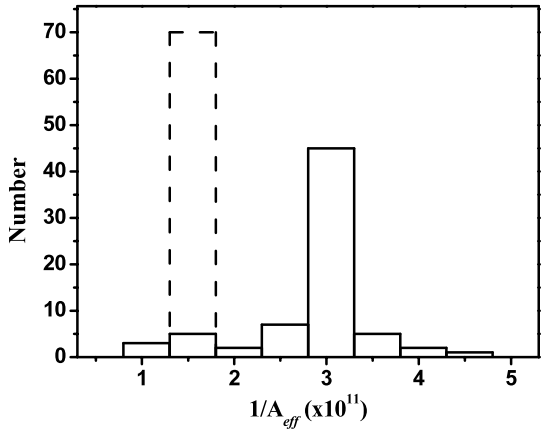

Fig. 5 Distribution of finding $1/A_{\text{eff}}$, initiation and after 10,000 round trips, for a cavity tuning range of 70 μm

the chaotic state with a strange attractor to a quasi-periodic state, and then converges to a fixed point. After long time evolution, the nonlinear Kerr coefficient γ does adapt to the edge of chaos.

Acknowledgement This work is supported by the Natural Science Council of Taiwan, Republic of China, under grant NSC 96-2628-E-009-018-MY3.

References

1. P. Melby, J. Kaidel, N. Weber, A. Hübler, Adaptation to the edge of chaos in the self-adjusting Logistic map. Phys. Rev. Lett. **84**, 5991 (2000)
2. P. Melby, N. Weber, A. Hübler, Dynamics of self-adjusting systems with noise. Chaos **15**, 033902 (2005)
3. S.F. Elena, R. Sanjuan, RNA viruses as complex adaptive systems. Biosystems **81**, 31 (2005)
4. V.P. Zhigulin, M.I. Rabinovich, R. Huerta, H.D.I. Abarbanel, Robustness and enhancement of neural synchronization by activity-dependent coupling. Phys. Rev. E **67**, 021901 (2003)
5. V.P. Zhigulin, Multiple-scale dynamics in neural systems: Learning, synchronization, and network oscillations. Ph.D. Dissertation, Dept. of Physics California Institute of Technology (2004)
6. C.O. Weiss, W. Klische, On observability of Lorenz instabilities in lasers. Opt. Commun. **51**, 47 (1984)
7. C.O. Weiss, R. Vilaseca, *Dynamics of Lasers* (VCH, Weinheim, 1991), p. 241
8. L.A. Lugiato, F. Prati, L.M. Naducci, P. Ru, J.R. Tredicce, D.K. Bandy, Role of transverse effects in laser instabilities. Phys. Rev. A **37**, 3847 (1988)
9. L.A. Lugiato, G.L. Oppo, J.R. Tredicce, L.M. Narducci, M.A. Pernigo, Instabilities and spatial complexity in a laser. J. Opt. Soc. Am. B **7**, 1019 (1990)
10. G. D'Alessandro, G.L. Oppo, Gauss–Laguerre modes: 'a sensible' basis for laser dynamics. Opt. Commun. **88**, 130 (1992)
11. J.M. Greene, A method for determining a stochastic transition. J. Math. Phys **20**, 1183 (1979)
12. M.D. Wei, W.F. Hsieh, C.C. Sung, Dynamics of an optical resonator determined by its iterative map of beam parameters. Opt. Commun. **146**, 201 (1998)
13. M.D. Wei, W.F. Hsieh, Bifurcation of fundamental Gaussian modes in Kerr-lens mode-locked lasers. Opt. Commun. **168**, 161 (1999)
14. M.D. Wei, W.F. Hsieh, Cavity configuration dependent nonlinear dynamics in Kerr lens mode-locked lasers. J. Opt. Soc. Am. B **17**, 1335 (2000)
15. H.H. Wu, W.F. Hsieh, Observations of multipass transverse modes in an axially pumped solid-state laser with different fractionally degenerate resonator configurations. J. Opt. Soc. Am. B **18**, 7 (2001)
16. H.H. Wu, C.C. Sheu, T.W. Chen, M.D. Wei, W.F. Hsieh, Observation of power drop and low threshold due to beam waist shrinkage around critical configurations in an end-pumped Nd:YVO_4 laser. Opt. Commun. **165**, 225 (1999)
17. P.T. Tai, W.F. Hsieh, C.H. Chen, Direct generation of optical bottle beams from a tightly focused end-pumped solid-state laser. Opt. Express **12**, 5827 (2004)
18. P.T. Tai, W.F. Hsieh, H.H. Wu, Suppression of spatial hole burning in a solid-state laser with the degenerate resonator configuration. Opt. Express **13**, 1679 (2005)
19. C.H. Chen, P.T. Tai, W.F. Hsieh, Cavity-configuration-dependent instability in a tightly focused end-pumped solid-state laser. Opt. Commun. **241**, 145 (2004)
20. N.J. Halas, S.N. Liu, N.B. Abraham, Route to mode locking in a three-mode He–Ne 3.39-μm laser including chaos in the secondary beat frequency. Phys. Rev. A **28**, 2915 (1983)
21. D.Y. Tang, M.Y. Li, N.R. Heckenberg, U. Hubner, Chaotic dynamics of an optically pumped NH_3 multitransverse-mode ring laser. J. Opt. Soc. Am. B **13**, 2055 (1996)
22. D.E. Spence, P.N. Kean, W. Sibbett, 60-fsec pulse generation from a self-mode-locked Ti:sapphire laser. Opt. Lett. **16**, 42 (1991)
23. J.M. Shieh, F. Ganikhanov, K.H. Lin, W.F. Hsieh, C.L. Pan, Completely self-starting picosecond and femtosecond Kerr-lens mode-locked Ti:sapphire laser. J. Opt. Soc. Am. B **12**, 945 (1995)
24. D.G. Juang, Y.C. Chen, S.H. Hsu, K.H. Lin, W.F. Hsieh, Differential gain and buildup dynamics of self-starting Kerr lens mode-locked Ti:sapphire laser without an internal aperture. J. Opt. Soc. Am. B **14**, 2116 (1997)
25. J.H. Lin, W.F. Hsieh, Three-frequency chaotic instability in soft-aperture Kerr-lens mode-locked laser around 1/3-degenerate cavity configuration. Opt. Commun. **225**, 393 (2003)
26. T. Brabec, Ch. Spielmann, P.F. Curley, F. Krausz, Kerr lens mode locking. Opt. Lett. **17**, 1292 (1992)
27. T. Brabec, P.F. Curley, Ch. Spielmann, E. Wintner, A.J. Schmidt, Hard-aperture Kerr-lens mode-locking. J. Opt. Soc. Am. B **10**, 1029 (1993)
28. D. Cote, H.M. van Driel, Period doubling of a femtosecond Ti:sapphire laser by total mode locking. Opt. Lett. **23**, 715 (1998)
29. S.R. Bolton, R.A. Jenks, C.N. Elkinton, G. Sucha, Pulse-resolved measurements of subharmonic oscillations in a Kerr-lens mode-locked Ti:sapphire laser. J. Opt. Soc. Am. B **16**, 339 (1999)
30. J.H. Lin, M.D. Wei, W.F. Hsieh, H.H. Wu, Cavity configurations for soft-aperture Kerr-lens mode-locking and multiple period bifurcations in Ti:sapphire lasers. J. Opt. Soc. Am. B **18**, 1069 (2001)
31. D.H. Auston, Transverse mode locking. IEEE J. Quantum Electron. **4**, 420 (1968)
32. P.L. Smith, Mode-locking of lasers. Proc. IEEE **58**, 1342 (1970)
33. F. Krausz, T. Brabec, Ch. Spielmann, Self-starting passive mode locking. Opt. Lett. **16**, 235 (1991)
34. S.R. Bolton, M.R. Acton, Quasiperiodic route to chaos in the Kerr-lens mode-locked Ti:sapphire laser. Phys. Rev. A **62**, 063803 (2000)
35. B. Segard, S. Matton, P. Glorieux, Targeting steady states in a laser. Phys. Rev. A **66**, 053819 (2002)

36. G.L. Lippi, S. Barland, F. Monsieur, Invariant integral and the transition to steady states in separable dynamical systems. Phys. Rev. Lett. **85**, 62 (2000)
37. X. Hachair, S. Barland, J.R. Tredicce, G.L. Lippi, Optimization of the switch-on and switch-off transition in a commercial laser. Appl. Opt. **44**, 4761 (2005)
38. E. Ott, C. Grebogi, J.A. Yorke, Controlling chaos. Phys. Rev. Lett. **64**, 1196 (1990)
39. K. Pyragas, Continuous control of chaos by self-controlling feedback. Phys. Lett. A **170**, 421 (1992)
40. T. Shinbrot, C. Grebogi, E. Ott, J.A. Yorke, Using small perturbations to control chaos. Nature **363**, 411 (1993)
41. P. Grassberger, I. Procaccia, Characterization of strange attractors. Phys. Rev. Lett. **50**, 346 (1983)
42. H. Haken, Analogy between higher instabilities in fluids and lasers. Phys. Lett. A **53**, 77 (1975)
43. H. Risken, K. Nummedal, Self-pulsing in laser. J. Appl. Phys. **39**, 4662 (1968)
44. R. Graham, H. Haken, Quantum theory of light propagation in a fluctuating laser-active medium. Z. Phys. **213**, 420 (1968)
45. L.A. Lugiato, C. Oldano, L.M. Narducci, Cooperative frequency locking and stationary spatial structures in lasers. J. Opt. Soc. Am. B **5**, 879 (1988)
46. A.E. Siegman, *Lasers* (University Science Books, Mill Valley, 1986). Chap. 28
47. S.A. Collins, Lens-system diffraction integral written in terms of matrix optics. J. Opt. Soc. Am. **60**, 1168 (1970)
48. C.H. Chen, M.D. Wei, W.F. Hsieh, Beam-propagation-dominant instability in an axially pumped solid-state laser near degenerate resonator configuration. J. Opt. Soc. Am. B **18**, 1076 (2001)
49. P.F. Moulton, Spectroscopic and laser characteristics of Ti:Al_2O_3. J. Opt. Soc. Am. B **12**, 125 (1986)
50. J.F. Pinto, L. Esterowitz, G.H. Rosenblatt, M. Kokta, D. Peressini, Improved Ti:Sapphire laser performance with new high figure of Merit crystals. IEEE J. Quantum Electron. **30**, 2612 (1994)
51. J.N. Kutz, B.C. Collings, K. Bergman, W.H. Knox, Stabilized pulse spacing in soliton lasers due to gain depletion and recovery. IEEE J. Quantum Electron. **34**, 1749 (1998)
52. J.H. Lin, W.F. Hsieh, H.H. Wu, Harmonic mode locking and multiple pulsing in a soft-aperture Kerr-lens mode-locked Ti:sapphire laser. Opt. Commun. **212**, 149 (2002)
53. N.H. Packard, J.P. Crutchfield, J.D. Farmer, R.S. Shaw, Geometry from a time series. Phys. Rev. Lett. **45**, 712 (1980)
54. H. Haken, *Synergetics: An Introduction* (Springer, Berlin, 1985)
55. C.H. Chen, P.T. Tai, W.F. Hsieh, M.D. Wei, Multibeam-waist modes in an end-pumped Nd:YVO_4 laser. J. Opt. Soc. Am. B **18**, 1220 (2003)
56. M.C. Cross, P.C. Hohenberg, Pattern formation outside of equilibrium. Rev. Mod. Phys. **65**, 851 (1993)
57. A. Yariv, P. Yeh, *Photonics: Optical Electronics in Modern Communications* (Oxford University Press, New York, 2006), p. 635